ReMAP

Real-time Condition-based Maintenance for Adaptive Aircraft Maintenance Planning

REMAP – Deliverable D3.3
Sensors technical data package and reliability assessment

This project has received funding from the European Union's Horizon 2020 research and innovation programme under grant agreement No 769288

Grant Agreement No.	769288
Project Start Date	01-06-2018
Duration of the project	48 months
Deliverable Number	D3.3
Deliverable Leader	ENSAM
Dissemination Level (PU, CO, CI)	PU
Status	Draft
Submission Date	30/11/2020
Author (Institution) Email	Marc.rebillat@ensam.eu
Project website	https://h2020-remap.eu

This project has received funding from the European Union's Horizon 2020 research and innovation program under grant agreement No 769288.

Document History

Rev Nr	Description	Author	Review	Date
0.1	First Draft	Mikhail GUSKOV		01/02/2019
0.2	Second Draft	Marc REBILLAT		12/02/2019
0.3	Draft 3	Marc REBILLAT, Mikhail GUSKOV		21/03/2019
0.4	Updated in reply to T.L.	Marc REBILLAT, Mikhail GUSKOV		25/03/2019
0.5	Update by CTEC	Jocelyn REBUFA and Gladys JAUSSAUD		05/04/2019
0.6	Update by TUD	Dimitrios ZAROUCHAS		02/05/2019
1	Finalization for review	Marc REBILLAT		09/05/2019
1.1	Feedback from OPT	Marc REBILLAT		10/05/2019
1.2	ERT/EMT description	Marc REBILLAT		17/07/2019
1.3	ERT/EMT description, gluing process	Gladys JAUSSAUD		17/07/2019
2.0	Addition of results related with PZT	William BRIAND & Marc REBILLAT		04/06/2020
2.1	Addition of ageing results	William BRIAND		16/07/2020
2.2	Addition of time reciprocity results	William BRIAND		11/09/2020
2.3	First draft for WP3 dissemination	Marc REBILLAT		29/09/2020
2.4	Inclusion of UPAT and CTEC feedbacks	Marc REBILLAT		13/10/2020
2.5	Internal review	Pierre BIEBER & Marc REBILLAT		16/11/2020
2.6	Final review	Bruno Santos		24/11/2020

Index

Abbreviations

CTEC	Cedrat Technologies S.A.
CFRP	Carbon Fibre Reinforced Polymer
EMB	Embraer S.A.
EMT	Electro-Mechanical Test
ERT	Emission-Reception Test
ENSAM	Ecole Nationale Supérieure d'Arts et Métiers
OF	Optical Fiber
PZT	Piezoelectric Sensor
S/A	Sensor/Actuator
SHM	Structural Health Monitoring
TTC	Tensile Test Coupons
TUD	Delft University of Technology
UD	Unidirectional
UPAT	University of Patras

1. Introduction

1.1. Project Summary

ReMAP “Real-time Condition-based Maintenance for adaptive Aircraft Maintenance Planning” (hereinafter also referred as “ReMAP” or “the project”), is a European project started on the 1st of June 2018 and has a duration of four years. The project addresses the specific challenge to take a step forward into the adoption of Condition-Based Maintenance in the aviation sector. In order to achieve this, a data-driven approach will be implemented, based on hybrid machine learning & physics-based algorithms for systems, and data-driven probabilistic algorithms for systems and structures. A similar approach will be followed to develop a maintenance management optimisation solution, capable of adapting to real-time health conditions of the aircraft fleet. These algorithms will run on an open-source IT platform, for adaptive fleet maintenance management. The proposed Condition-Based Maintenance solution will be evaluated according to a safety risk assessment, ensuring its reliable implementation and promoting an informed discussion on regulatory challenges and concrete actions towards the certification of Condition-Based Maintenance.

1.2. Purpose of this Document

This document is the Deliverable D3.3 of the ReMAP Project. It addresses the definition of L-0 test articles and the reliability assessment of the piezoelectric and optical fiber sensors investigated in ReMAP.

The deliverable is part of Work Package 3 (Sensor Technologies for SHM) from the project. The work is related with the Task 3.5 (Sensors reliability assessment).

1.3. Context

Sensors reliability is a crucial issue in Structural Health Monitoring (SHM) and it is essential to ensure that sensors will function properly during the lifetime of the structure and do not jeopardize its integrity. Within this deliverable, the sensors and their connecting components will be subjected to realistic operational and environmental conditions to assess their reliability status. To achieve this goal, sensorized coupons will be analyzed in terms of stability and then submitted to repeated varying loads and temperature conditions as well as to ageing. Emphasis will be given to the performance of bonding between the sensors and the structure, as high-integrity bond should be maintained during the SHM in service use. Two types of sensors will be under study: piezoelectric (PZT) and optical fibers (OF). Self-diagnostic capabilities will be developed to monitor the performances of the PZT elements and to ensure that the sensors’ output will remain reliable. Measurement repeatability will be used to assess OF correct bonding. Regarding PZTs, the tests will be performed at ENSAM and CTEC will bond PZTs and detail the associated gluing procedure. Regarding OFs, tests will be carried out at TUD and OF sensors will be provided by SMARTEC. Ageing tests with both OF and PZT will also be carried out at TUD and PZTs bonded on tested coupons will be regularly tested by ENSAM. Based on the results of those tests TUD, SMARTEC, CTEC and ENSAM will propose and implement possible improvements to the sensors packaging and installation procedures.

2. L-0 test articles definition

2.1. L-0 coupons description

The level 0 (L-0) coupons are designed for qualifying the PZT and OF assembly on the substrate part. The core principle of the approach is to subject the coupon with glued PZT and OF to thermal and mechanical loads typical of aeronautic environment and to verify PZT electromechanical properties and OF reception properties that should remain sensibly identical to the initial state. Thus, L-0 specimens are shaped as tensile test coupons (TTCs), realized in typical structural material and offering enough room for sensors installation.

The test specimen is a rectangular tensile coupon. The material selected is a graphite-epoxy IM7/8552 with properties obtained by its datasheet from Hexcel® (Table 1). The coupon is made up with 2 stacking cases (UPAT skin and EMB as described in Table 2) composed of 3 zones: central part of size 4Dx12D (D standing for the PZT diameter – chosen as 20 mm) and of two taps at the ends for fixing the coupon in the test machine grips, as shown in Figure 1. Note that the total thickness of the specimen, including taps, should not exceed 8 mm to fit with the test machine grips. The testing will mostly be carried out on the reduced layup material (UPAT skin) but the other stacking cases are also included to analyze the transferability on actual real materials.

Table 1 - Mechanical properties of **IM7/8552** given by Hexcel®

Property	IM7/8552 UD
Density [g/cm^3]	1.57
0º Tensile Modulus [GPa]	163
90º Tensile Modulus [GPa]	10
0º Tensile Strength [MPa]	2538
90º Tensile Strength [MPa]	92
0º Compression Strength [MPa]	1690
In-plane Shear Strength [MPa]	106

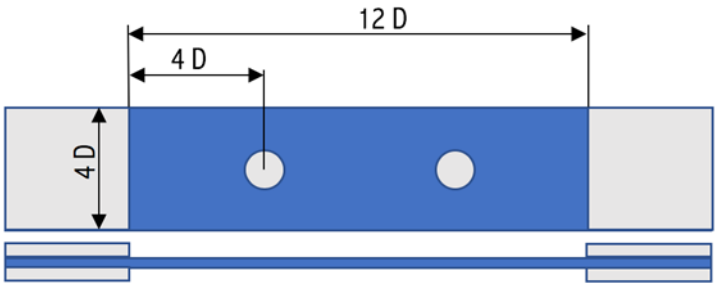

Figure 1: L-0 coupon design schematic

Table 2 – Lay-up configurations used in numerical analysis

	UPAT	2 x UPAT	EMB
Skin	$[45^F/0/45/90/-45/0]_s$	$[45^F/0/45/90/-45/0]_{2s}$	$[45^F/0/45/90/-45/0_2/45/90/-45/0_2/45/90/-45/0/45/-45]_s$.
Stiffener	$[45^F/0/45/-45]_s$	$[45^F/0/45/-45]_{2s}$	$[45^F/0_3/45/90/-45/0/-45/0/45/0]_s$.
Nominal Thickness	1.71 (skin) 1.18 (stiffener)	3.42 (skin) 2.36 (stiffener)	4.85 (skin) 3.28 (stiffener)

As stated above, two material cases are considered (UPAT and EMB skin according to Table 2). A set of UPAT skin coupons should be manufactured to enable the sample characterization (2 coupons for destructive tensile testing) and the reliability testing *per se* (4 UPAT coupons for nominal reliability test protocol) and to have a set of spare samples for backup. Two additional coupons of EMB layup are intended for assessing the transferability of the PZT and OF coupling to the L-2 case.

2.2. Piezoelectric elements description and associated bonding procedure

The PZT patches have been selected regarding the following criteria:

- Compatible with the LWDS electronics specification
- Maximize the generation and reception of lamb waves in the frequency range of interest

For these reasons, the piezo type that has been selected is a **PZT-5 disc of diameter 20mm and thickness 0.5 mm**. Selection justification is given in the following paragraphs.

2.2.1. LWDS specification

In order to be compatible with the LWDS the piezo patch needs to operate in quasi-static state, i.e. non-resonant. The first resonance frequency of the selected patch is around 4.1 MHz.

The capacitance of the patch needs to be minimized for the LWDS electronics. For the selected patch the capacitance is 8.2 nF.

2.2.2. Maximizing emission and reception of Lamb waves

The propensity of a piezoelectric patch to excite or to sense Lamb waves would depend on the electromechanical coupling in the material and on the shape of the patch, linked to the substrate structure material (especially the latter's propagative properties).

Maximizing the coupling of a patch is related to improving the d_{31} coefficient. For the selected patch the d_{31} coefficient is -208 pC/N. This material has also been chosen in many publications (APC850 [1] [2], PIC-151 , [3], NCE51 [4]).

Another important parameter is the patch diameter. For a diameter of 20mm dispersion curves, for composite material used in REMAP, have been traced and the coupling quality has been highlighted (see Appendix 2). For a given materiel, and thickness of the sample, the coupling varies with the frequency of the waves.

2.2.3. Gluing process description

As for the patch selection, the gluing process must enhance the coupling between the patch and the sample. Glass beads of 50µm diameter are used to obtain a thin and homogenous glue layer.

The Epoxy glue Loctite EA9492 has been selected for having a high shear strength ($20\ N/mm$ below $70°C$), short cure time ($24h\ at\ 22°C$) and a low pressure needed for curing.

To protect the patches and the piezoelectric element, the sealant "Dow corning 3145" has been selected as a coating. This product shows a high tensile strength (6.5 MPa) and elongation (600%), with ambient curing temperature (63 min at 25°C).

Patch preparation	Secure wire weld with glue (3M DP490) and cure at 70°C for 1h
Support preparation	Slightly polish the support with an abrasive sheet (the operator has to wear mask and gloves).

	Clean the surface with ethanol
Glue preparation	Mix glass beads of 50 µm diameter with the glue (EA9492) to force a homogeneous glue layer of 50 µm
Gluing	Drop a small quantity of glue on the support
	Apply the patch on the glue with a spiral movement to homogenize the glue layer
	Clean the surface and insert a paper sheet to protect the patch
	Maintain the patch on position during 24h

2.3. Optical fibers description and associated bonding procedure

2.3.1. SMARTape attachment concept

Figure 2: Inside the 3D printer after the adhesive layer was printed

A thin layer, approximately 0.2mm, of a co-polyamide from Griltex® is deposited on one side of the SMARTape using a 3D printer. The Griltex® is in the form of thread and is placed inside the extrusion head. The temperature on the bed of the printer is 85°C while the extrusion head is at around 220°C. A dummy tape was first used to make sure the CFRP can withstand the process and the associated temperatures. For the subsequent bonding, direct heat and pressure is applied using a heated metallic plate. The metallic plate has two indents at the position of the two optical fibers to prevent the plate from moving while applying the pressure over the SMARTape. A thermocouple is attached to the plate's lower surface to measure the temperature and controller sends a signal to a resistance to turn on or off depending on the temperature. It was concluded that the adhesion quality is good when ~140°C are applied for 20-30 seconds. It is also observed that preheating the surface provides better adhesion quality. Detaching the tape from the coupon is relatively easy.

For the actual SMARTape, the thermoplastic layer is applied at the thick part of the CFRP SMARTape. The tape is then bonded to the panel using the following steps:

- The area to be bonded is first gritted using sandstone paper and the surface is cleaned with acetone.
- The panel's surface is preheated using a heat gun, until the stiffener side is barely touchable with bare hands.
- A heat source (heat plate at approximately 140^{o} C) is used to preheat the plate's surface.
- The SMARTape is placed on the surface and the edges are taped so it stays in place.
- The heat plate is placed over the SMARTape and pressure is applied. Because the heat plate's length is smaller than the SMARTape's length, the heat plate is moved over the SMARTape, in order to bond the full surface.
- At each step, the heat is applied for approximately 20-30 seconds.
- In places where we observe that the bonding is insufficient heat and pressure are reapplied.

The final outcome is as shown in Figure 2.

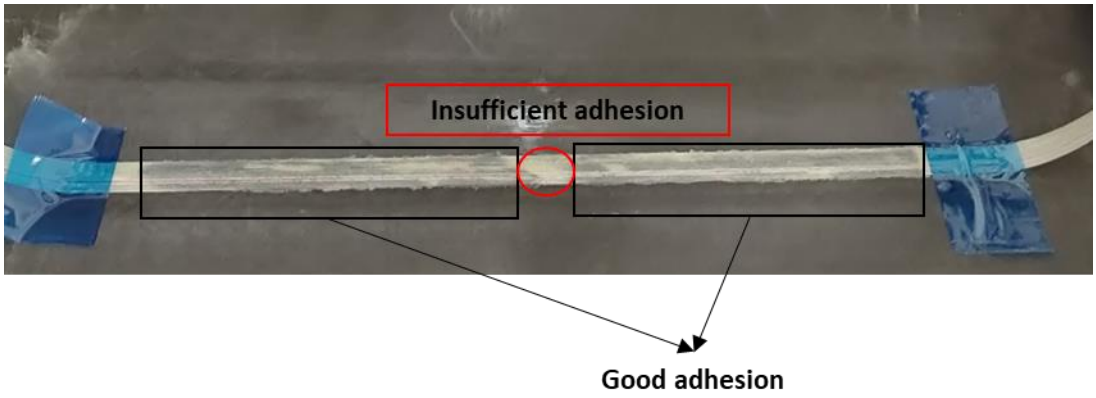

Figure 3: SMARTape after adhesion to the panel skin

3. Reliability testing approach

The sensor/actuator reliability testing would consist of a sequence of thermal, mechanical and humidity conditions on L0 and piezoelectric element assemblies to track potential deviations in the sensor properties during the procedure. The idea of this approach is issued from the recent experience of the previous research projects at PIMM. The primary goal of this testing is to verify the operation of bonded PZT sensors/actuators after the application of environmental conditions (hot / cold / wet atmosphere, substrate structural strain). Practical validation criteria for the piezoelectric element is the capacitance discrepancy below a tolerance threshold and the correlation coefficient between successive emission-reception tests.

The reliability testing of the Optical Fibers (OF) consists of mechanical fatigue tests on L0 coupons and ageing process of the OF solely and bonded on the L0 coupons. This way the durability of the OF against ageing and the consistency in measuring strain will be tested. Practical validation criteria for the OF and the measurements will be that signal's noise (error of measurements) during the fatigue and after each ageing period will be consistent within 5%, meaning that the strain should remain constant throughout the fatigue test and between the different ageing states as long as there is no damage at the structure.

3.1. Raw coupon characterization and history notices

The first step consists in identifying and documenting each coupon to be able to follow during its lifetime the sequence of tests endured by a given coupon. Thus, a history notice (see Appendix 9) will be associated with each coupon and will be filled out when receiving the coupon or when performing any test on it. Among the various information to be collected, a picture of the coupon will be taken, its weight and dimensions will be measured, and a unique identification number will be associated with it.

3.2. Destructive tensile tests

Destructive tensile tests will be carried out on 2 coupons. These tensile tests will allow assessing the material properties, especially the elasticity modulus and subsequently the load corresponding to the target strain level associated with the nominal reliability test protocol.

3.3. Nominal reliability tests protocol for piezoelectric elements

The nominal reliability protocol consists of a sequence of operations that are depicted in the following table and will be applied on 4 coupons with the UPAT material and 2 coupons of the EMBRAER material. The details of the tests MT, EMT and ERT are given after the table.

Table 3: Test protocol for piezoelectric elements

A		Coupons and PZT elements reception at CTEC and bonding		
A.1		Coupon reception at CTEC	Identification number, picture, weight, dimensions	
A.2	EMT1	PZT element reception at CTEC	Identification number, free EMT, weight, dimensions	
A.3	EMT2	PZT element bonding	Picture, weight and EMT after bonding	
A.4	ERT0	Emission-reception test	ERT	
A.5		Coupon sending to ENSAM		
B		Reliability testing at ENSAM		
B.1		Coupon reception at ENSAM		
B.2	EMT3	Electromechanical test	EMT	DAY 1
B.3	ERT1	Emission-reception test	ERT	
B.4	MT1	Mechanical test at ambient temperature	100000 cycles @ 10 Hz (≃3 h) @ 0.1% of deformation at ambiant temperature	
B.5	EMT4	Electromechanical test	EMT	
B.6	ERT2	Emission-reception test	ERT	
B.7	HWC	Hot and wet environment	10 cycles from ambient to 70°C and 75 % of humidity during T_{stab} minutes (≃ 30 min)	DAY 2
B.8	EMT5	Electromechanical test	EMT	DAY 3
B.9	ERT3	Emission-reception test	ERT	
B.10	MT2	Mechanical test at ambient temperature	100000 cycles @ 10 Hz (≃3 h) @ 0.1% of deformation at ambient temperature	
B.11	EMT6	Electromechanical test	EMT	
B.12	ERT4	Emission-reception test	ERT	

Additional notes regarding tests to be carried out:

- **MT**: Mechanical tests will be carried out on a 50kN Instron Tensile testing machine, at temperatures of -40°C / 20°C / 70°C (temperature range corresponding to the properties of the glue, as indicated by CTEC) and up to a given strain level ε_0 (order of magnitude corresponding to the fatigue strength of the substrate material, the order of magnitude is $\varepsilon_0 \approx 0.1\%$). Note that the total thickness of the specimen, including taps, should not exceed 8 mm to fit with the test machine grips.
- **EMT**: Electromechanical tests will be carried out with a HIOKI LCR meter IM3533 test between $1\,\mathrm{kHz}$ and $150\,\mathrm{kHz}$ at 20°C at 1V and over 801 measurements points and 4 repetitions will be performed.
- **ERT**: Emission-Reception tests consists of 10 successive repetitions of a $N_c = 5$-cycles tone burst $x(t)$ with a central frequency $f_0 = 150$ kHz, an amplitude $A = 10V$ at 20°C and defined as follows:

$$x(t) = A\sin(2\pi f_0 t)\sin\left(\frac{\pi f_0 t}{N_c}\right) \text{ for } 0 < t < \frac{N_c}{f_0}$$

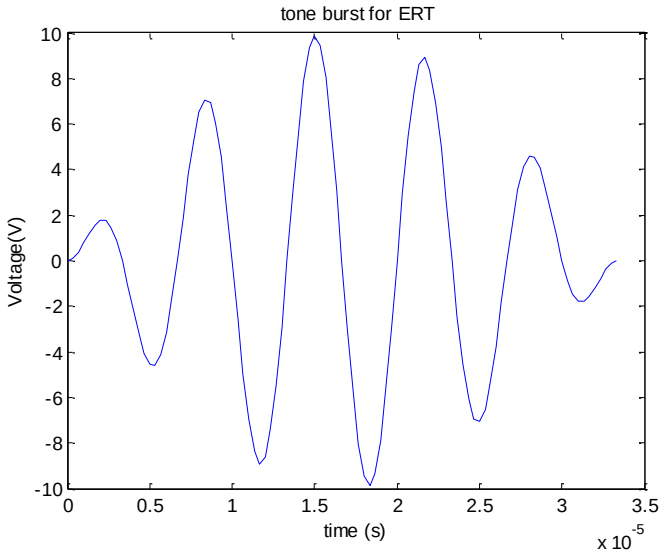

Figure 4: Tone burst for ERT (1 iteration)

3.4. Nominal reliability tests protocol for optical fibers

The nominal reliability protocol of OF consists of the following 2 tasks as presented in Table 4.

Table 4: Reliability protocol of OF

Test Case	Condition	Duration	Check	Number of coupons
1. Mechanical fatigue tests	Displacement control 0.1% strain/Ambient conditions	300k cycles	With Digital Image Correlation	3 L0
2. Optical Fibre ageing	35 C, 95% humidity	6, 12, 24 weeks	With Digital Image Correlation	3 OF per duration

Test Case 1 – Mechanical fatigue tests

3 L0 coupons will be tested under tension-tension (T-T) fatigue loading, with fatigue ratio $R = 0.1$, under displacement control with 0.1% δmax of the strain failure. One OF will be permanently attached to one side of the L0, along its length, while on the other side a speckle pattern will be applied for a full-field surface strain measurement using digital image correlation technique. Every 1000 cycles the fatigue test will be interrupted and the L0 will be loaded quasi-statically with displacement rate 1.5mm/min under displacement control to δmax to acquire the data from the two techniques.

Test case 2 – Optical fiber ageing

9 OFs will be placed in a conditioning chamber subjected to $35°C$ and 95% relative humidity. These conditions are selected based on ASTM B 117 – Standard Practice for Operating Salt Spray (fog) Apparatus. 3 OFs will be removed after 6,12,24 weeks respectively and will be attached using the smart-tape concept to one side of the L0 coupon along its length while one the other side a speckle pattern will be applied for strain measurement, similar to the previous test case. Then the L0 coupon will be loaded quasi-statically with displacement rate 1.5mm/min up to 0.1% strain of the tensile failure strain and digital image correlation technique will acquire pictures. After the test, the OF will be removed from the specimen and the next ones will be attached following the same procedure. These tests will be repeated 3 times, at 6,12,24 weeks.

3.5. Nominal reliability tests protocol for Optical fibers and PZT elements as sensing network

The aim of this test protocol is to create a sensing network with OFs and PZTs and check if there is an interaction between the measurements of the two different sensing types during the mechanical and ageing process. A similar procedure as the test case 2, described in 3.4, will be followed. An overview of the test is given in Table 5.

Table 5: Reliability test protocol for OF & PZT

Test Case	Condition	Duration	Check	Number of coupons
1. Optical Fibre and PZT ageing	35 C, 95% humidity	6, 12, 24 weeks	With Digital Image Correlation and the baseline waveforms	3 L0 per duration

PZTs and OFs will be permanently attached at L0 coupons using the same structural adhesive. Initially, emission-reception and electromechanical tests will be performed at the 9 pristine/non-aged L0 coupons to acquire baseline data. These measurements will be performed at ENSAM and then the coupons will be sent to TU Delft where the OFs will be attached and a speckle pattern will be applied. The L0 coupons will be loaded quasi-statically with displacement rate 1.5mm/min up to 0.1% strain of the tensile failure strain and digital image correlation technique will acquire pictures for strain analysis. Afterwards, the specimens will be placed in the conditioning chamber subjected to $35\,°C$ and 95% relative humidity. After 6,12 and 24 weeks, 3 coupons will be removed sequentially from the chamber and the same quasistatic (@TU Delft) and emission-reception and electromechanical (@ENSAM) tests, as before the ageing, will be performed.

4. Destructive tensile tests results

4.1. Objective of the experiment

To correctly perform the tests for piezoelectric elements and optical fibers, mechanical properties of the L0 coupons need to be assessed. That is why destructive tensile tests will be carried out on 2 samples. The material properties that will be assessed in this experiment are:

- The elasticity modulus
- The tensile strength

4.2. Experimental devices

A MTS tensile machine with a maximum load of 100kN has been used to perform these experiments. It is equipped with sensors to track traverse displacement and stress. The strain is measured by a video correlation technique. 4 reference points are painted on the surface of the sample under testing. The sample is recorded during the experiment with a camera. The recording and the tensile machine procedure start at the same time. A Python script then post-process the video to extract the position of the center of each for each frame. The strain of the sample is computed from these positions.

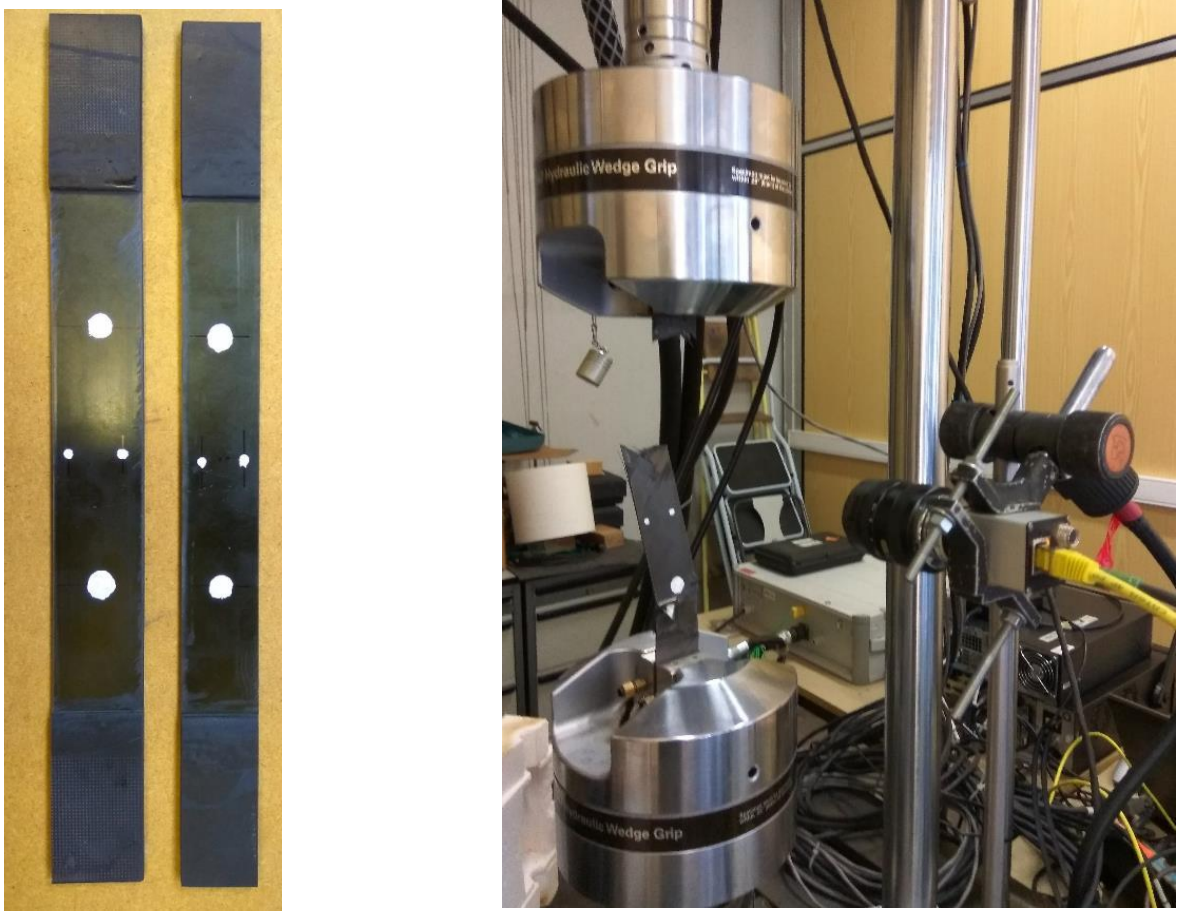

Figure 5 - Destructive test setup

4.3. Coupons description

L0 coupons are rectangular plates equipped with two tabs. The material selected is a graphite-epoxy IM7/8552. The material selected is a graphite-epoxy IM7/8552 with properties obtained by its datasheet from Hexcel® (Table 1). The coupon is made up of UPAT skin stacking case (Table 2). Since L0 coupons are too large to be broken by the $100kN$ tensile machine, it is split in two parts to reduce the section of the coupon and by so, the failure load.

The dimensions of a L0 coupon are given below.

Coupon ID	Width [mm]	Length [mm]	Thickness [mm]
L0-05 #1	42	400	1.9
L0-05 #2	36	400	1.9

4.4. Experimental protocol

For each coupon under testing, the coupon is placed at the center of the grips of the tensile machine. The destructive tensile procedure starts (tensile speed: 1mm/min) in the tensile machine and the video record starts at the same time. The test goes on until the failure of the sample. The video is then post-processed to get the strain. Finally, the stress versus strain graph is plotted to get the needed material properties.

4.5. Results and analysis

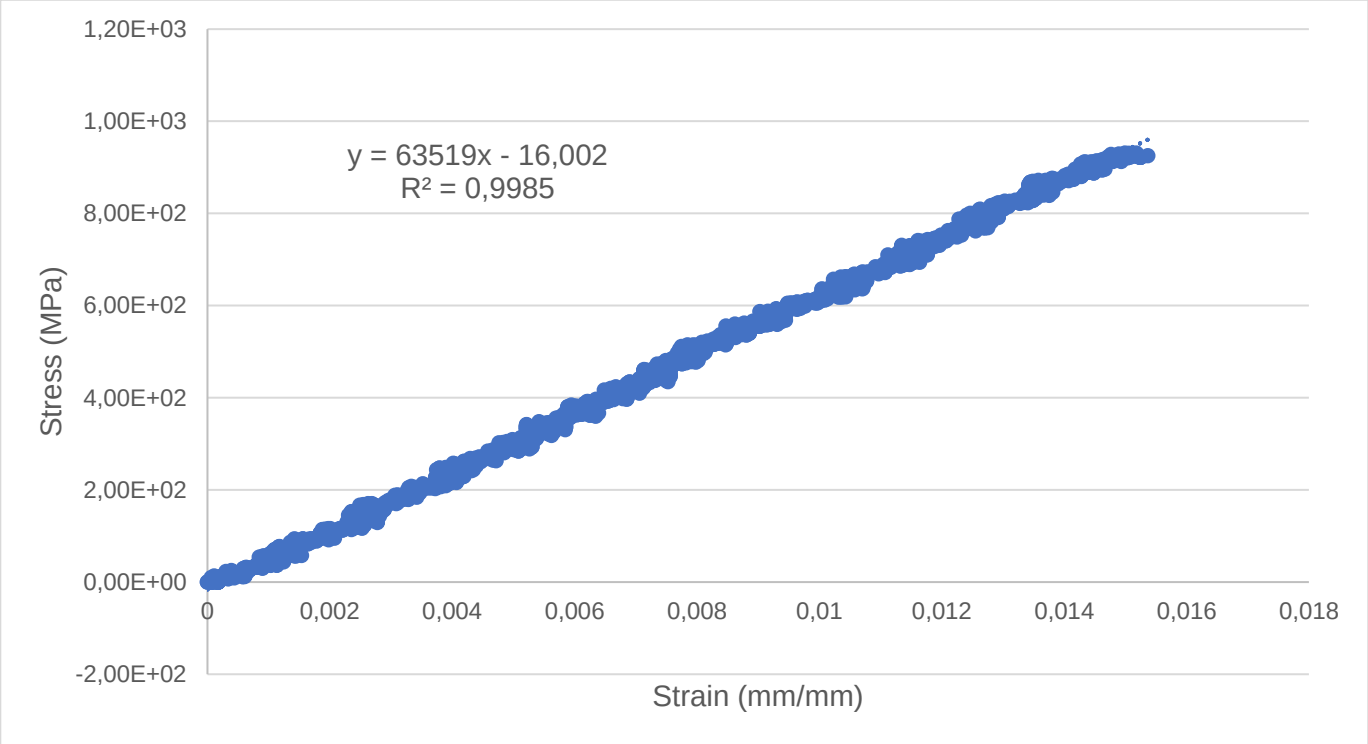

Figure 6 - Stress vs strain curve for the sample L0-05 #1

Mean values found between the 2 samples:

Coupon	**L0-05 #1**	**L0-05 #2**
Young modulus [GPa]	63.5	61,3
Tensile strength [MPa]	931	938

5. PZT element self-diagnostic and associated results

The objective of the present deliverable is to demonstrate that PZT elements stay bonded to their host structure and are not damaged while experiencing thermal and mechanical solicitations representatives of aeronautic operational conditions. This section introduces the procedure followed for PZT elements to perform self-diagnostic with respect to their bonding or damaged state.

5.1. Piezoelectric element self-diagnostic procedure

The PZT elements self-diagnostic procedure proposed here is based on PZT elements static capacitance, which can be estimated from the imaginary part of its electromechanical impedance. The efficiency of this recent procedure has already been demonstrated experimentally and appears to be sensitive to both bonding issues and to partial or total PZT element damaging. [5, 6, 7, 8, 1, 9]. Furthermore, this procedure has already been used in an aeronautical context [10, 11, 12]. This explains why this procedure has been retained for the REMAP project and is briefly recalled in what follows.

5.1.1. Admittance of a free piezoelectric element

The electrical admittance of a piezoelectric element $Y(\omega)$ is defined as the inverse of its electrical impedance $Z(\omega)$, i.e. the ratio (in the frequency domain) between the current $I(\omega)$ and the voltage $V(\omega)$ across the considered element. When the piezoelectric element undergoes free boundary conditions (i.e. when it is not bonded to any mechanical structure), its admittance $Y_l(\omega)$ is given by:

$$Y_l(\omega) = \frac{1}{Z(\omega)} = \frac{I(\omega)}{V(\omega)} = i\omega \times \frac{S}{t} \times \epsilon_{33} = i\omega C_l \qquad \text{Eq. (1)}$$

$V(\omega)$ is the voltage applied to the piezoelectric element and $I(\omega)$ is the resulting current. Moreover S and t are the area and the thickness of the considered element and ϵ_{33} stands for the dielectric constant of the constitutive material of the piezoelectric element. The static capacitance of the free piezoelectric element is here denoted as C_l.

5.1.2. Admittance of a piezoelectric element bonded on a host structure

If now a piezoelectric element bonded to a mechanical host structure is considered, its admittance $Y_c(\omega)$ is, under some assumptions validated in the low frequency range, a function of the mechanical impedance of the host structure $Z_s(\omega)$ and that of the piezoelectric element $Z_a(\omega)$:

$$Y_c(\omega) = i\omega C_l \left[1 - \kappa^2 \times \frac{Z_s(\omega)}{Z_s(\omega) + Z_a(\omega)}\right] \qquad \text{Eq. (2)}$$

κ^2 stands for the electromechanical coupling coefficient between the piezoelectric element and its host structure and can take values between 0 and 1. When the mechanical impedance of the host structure can be considered much greater than the one of the considered piezoelectric element, which is practically the case in the low frequency range, the previous equation can be rewritten as follows:

$$Y_c(\omega) = i\omega C_l[1 - \kappa^2] = i\omega C_c \qquad \text{Eq. (3)}$$

Here C_c stands for the static capacitance of the piezoelectric element once bonded to its host structure.

5.1.3. Piezoelectric element self-diagnostic procedure

The piezoelectric element self-diagnostic procedure used here is based on Eq. (1) and Eq. (3). From these equations, it appears, clearly, that the admittance of a piezoelectric element bonded to a given host structure is clearly depending on the element geometry (S,t) and on its electromechanical coupling coefficient κ^2. Thus, a healthy piezoelectric element correctly bonded to its host structure will have the following static capacitance:

$$C_c = \frac{S}{t} \times \epsilon_{33} \times [1 - \kappa^2] \qquad \text{Eq. (4)}$$

In practice, if the piezoelectric element itself is being damaged, this will cause a reduction of its area S or of its dielectric coefficient ϵ_{33}. Thus the product $S\epsilon_{33}$ will become $\alpha S\epsilon_{33}$ with $0 < \alpha < 1$. A a consequence, a damaged piezoelectric element will have the following capacitance :

$$C_c^E = \frac{\alpha S\epsilon_{33}}{t} \times [1 - \kappa^2] = \alpha C_c < C_c \qquad \text{Eq. (5)}$$

Following this observation, any damage occurring on the piezoelectric element itself can be identified by monitoring its static capacitance and by checking if it is diminishing. Once the piezoelectric element is totally damaged, its static capacitance will be drastically reduced.

Once a piezoelectric element will debond from its host structure, its electromechanical coupling coefficient κ will be reduced and become $\beta\kappa$ with $0 < \beta < 1$. The static capacitance of a piezoelectric element that is partially debonded is then given by :

$$C_c^D = \frac{S}{t} \times \epsilon_{33} \times [1 - (\beta\kappa)^2] > C_c \qquad \text{Eq. (6)}$$

As a consequence, any debonding occurring between the piezoelectric element and its host structure may be identified by monitoring again its static capacitance and especially if it increases. For a totally debonded piezoelectric element, its static capacitance will increase toward its static capacitance as a free element, i.e. C_l, see Eq. (1).

5.1.4. Piezoelectric element debonding or damaging criterion

It is demonstrated in the previous section that damaging or debonding of the piezoelectric element will manifest as variations of its static capacitance. Any variation (increase or decrease) of the static capacitance of the piezoelectric element over a previously set threshold will thus be the consequence of damage or a debonding occurring at the level of the piezoelectric element following a given environmental or operation solicitation. This threshold is chosen here as equal to 5%. Any variation of the static capacitance of a piezoelectric element higher than this threshold will thus be interpreted as a sign of damage or of debonding of the piezoelectric element. By denoting C_C the static capacitance of the piezoelectric element after its first bonding, and $\tilde{C}$ its current static capacitance, we thus consider that a significative event (debonding or damage) has happened if :

$$\frac{|\Delta C|}{C_c} = \frac{|\tilde{C} - C_c|}{C_c} > 5\% \qquad \text{Eq. (7)}$$

5.1.5. Emission-Reception test analysis

In addition to the piezoelectric element self-diagnostic procedure, emission-reception test will be carried out in order to validate the ability of a set of PZT pair to be able to send and receive signals in a consistent way when enduring reliability test. Each of the two PZT elements bonded on a given coupon will act sequentially as an actuator and a sensor. The signals measured during the first emission-reception test will be considered as reference signals and denoted as $R_n(t)$ where n stands for the actuator number. The signals collected during any upcoming emission-reception test will be denoted $T_n^i(t)$ where n stands again for the actuator number and i represents the emission-reception test number.

On the basis of these signals, the correlation coefficient $C_{i,n}$ for the emission-reception test number i and the PZT element number n will be computed as follows:

$$C_{i,n} = 1 - corrcoeff[R_n(t), T_n^i(t)]$$

We thus consider that a significative event (debonding or damage) has happened if:

$$C_{i,n} > 5\%$$

5.2. Results

5.2.1. Deviations from the initial protocol

- MT1 and MT2 targeted a sample strain of 0.1%. However, the tensile machine is driven in terms of transverse displacement and not in terms of the sample under study's strain. Indeed, due to the tensile stiffness, the strain computed from the transverse displacement is different from the strain of the coupon under study. To take this stiffness into account, a set of tests were performed on L0 coupons without PZTs to assess the multiplication coefficient between transverse displacement and strain of the sample. These experiments consisted in imposing a displacement and recording the associated strain. To record the strain of the sample, the same image correlation technique as used for the destructive tests, was performed. Finally, the measured strain versus imposed displacement graph is plotted and is used to determine the multiplication coefficients between the two quantities. These experiments were performed on both EMB and UPAT materials. For mechanical tests MT1 and MT2, the coefficients obtained from UPAT material are used for both types of L0 coupons.

- During the MT1 test, it appeared that the frequency of the fatigue test (10Hz) imposed in this document was too high for the controller of the fatigue machine. Indeed, for this test the amplitude of the command was a strain of 0.07% instead of 0.1%. In the second fatigue test (MT2) this issue is solved by decreasing the frequency from 10Hz to 4Hz.
- During HW test, the first cycle in the oven lasted more than expected: 90min instead of 30min.
- During MT2, the coupon L0-14 faced an unexpected buckling that probably damaged the sample (fibers crack sound was heard).

5.2.2. Typical EMT and ERT results

Typical Lamb wave emission/reception signals and impedance curves are shown in Figure 7.

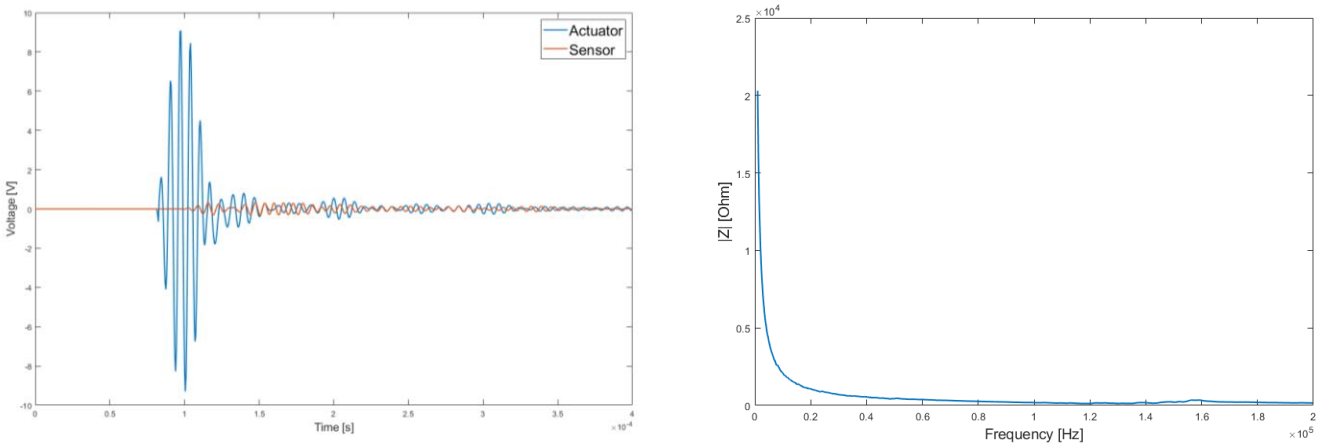

Figure 7: Typical results for ERT (left) and EMT (right) tests.

5.2.3. Admittance results

Admittance measurements have performed on free PZTs and after gluing on pristine coupons by CTEC (denoted respectively PZT_CTEC and Healthy_CTEC) as previously described. Then ENSAM performed the same test before testing (denoted as Healthy_ENSAM) and after each test (MT1_ENSAM, HW_ENSAM, MT2_ENSAM). Please refer to Table 3 for more details. The first thing to notice is that the static capacitance of a bonded PZT is lower than a free PZT as it can be seen in Figure 8. This is an expected theoretical result as described in Section 5.1 of this document.

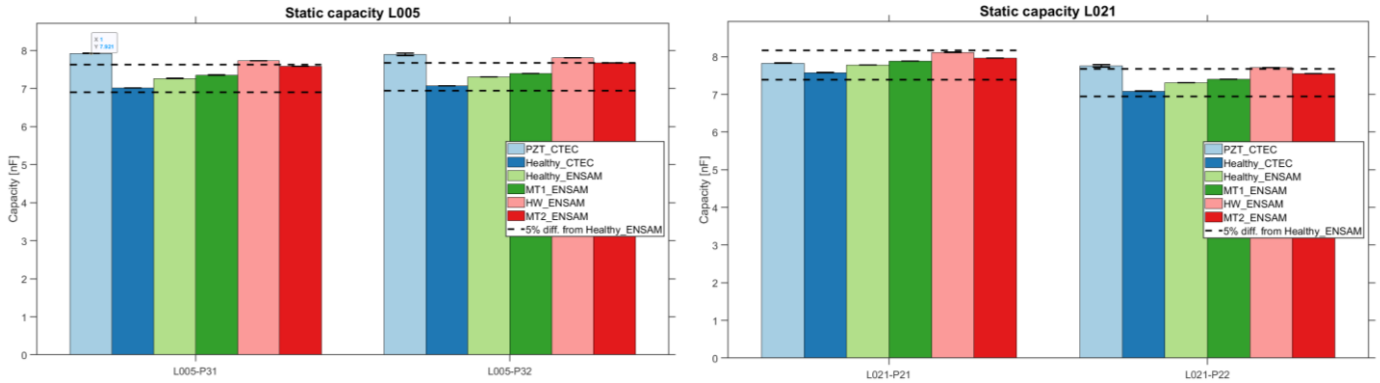

Figure 8: Static capacitance in nF of PZT P31 and P32 of L0 coupon 05 (EMB material) [left] and of each PZT P21 and P22 of L0 coupon 21 (UPAT material) [right]

Another phenomenon to notice is the difference of the static capacitance between the test Healthy_CTEC and Healthy_ENSAM. Since the coupon is the same between these two measurements and only travelled from CTEC to ENSAM, the results should be equal. This difference is probably due to the different experimental setup between the

two sets. Indeed, the wires used in the experiments have their own admittance that can influence the result. Since the ENSAM experimental setup remained the same during the entire test campaign, the reference case used for the rest of the study will be Healthy_ENSAM.

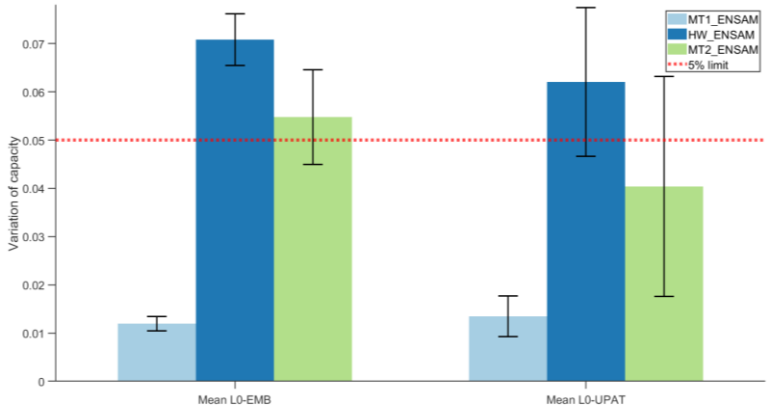

Figure 9: Variation of static capacitance from the healthy state Healthy_ENSAM. Mean L0-EMB (respectively Mean L0-UPAT) is the mean variation for all PZT glued on EMB coupons (respectively UPAT coupons).

It can, furthermore, be observed that the static capacitance increases only slightly after MT1 tests (about 1% on average according to Figure 9). This rise may be due to a very small debonding of the PZT from the surface of the coupon. This is encouraging since it shows that the selected glue along with the gluing process is strong enough to withstand the fatigue test of L1 coupons. Unfortunately, the measures after the Hot and Wet test (HW_ENSAM) show a much larger increase that is above the 5% limit imposed in this deliverable. This may indicate that the glue and the gluing process are not appropriate for real flight conditions i.e. when facing realistic high temperature and humidity conditions. A possible solution can come from structural bonding solutions used on analogous hosting aircraft components. Finally, after the MT2 test, a small static capacitance decrease can be observed. Although the magnitude of this latter transition appears near the variability of observations, this trend, observed for both specimen materials, might suggest that the hot/wet conditions impact can evolve over longer time scales. This track, as well as alternative gluing solutions, might provide subjects of future investigations, beyond REMAP framework.

5.2.4. Emission/reception results

Emission-reception tests were performed after PZT gluing on pristine coupons by CTEC (respectively Healthy_CTEC). Then ENSAM performed the same test before testing (Healthy_ENSAM) and after each test (MT1_ENSAM, HW_ENSAM, MT2_ENSAM). To compare the results with the same devices, only the data coming from ENSAM tests are used here. To compute the correlation coefficient, for each PZT, each state (actuator or sensor) and each repetition, the studied signal is compared to each repetition of the same configuration in the Healthy_ENSAM pristine case. Figure 10 shows the mean coefficient of every PZTs for each material with an error bars corresponding to the standard deviation.

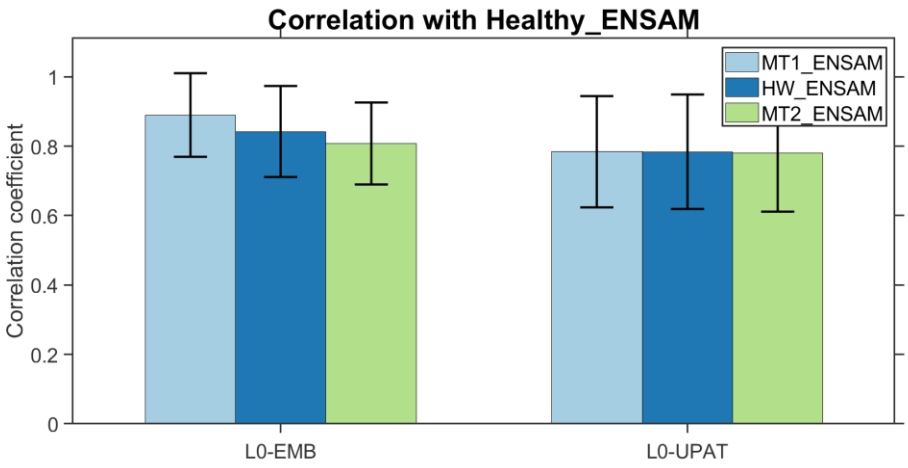

Figure 10: Correlation coefficients after the ERT tests.

The correlation coefficients generally stay relatively close to one, meaning that ERT tests are generating signals that are resembling each other's. For EMB coupons, the correlation coefficient slightly decreases between MT1 and HW, but without any statistical significance. It decreases again with the same order of magnitude between HW and MT2, again without being statistically significant due to high variability. It is, however, some kind of an expected result since the bonding of the PZT become weaker as the tests progress as seen from the static capacitance results. On the other hand, for UPAT coupons the mean coefficient does not vary throughout the test campaign. This is unexpected since the variation of capacitance indicates that the PZT bonding is weaker after the MT2 test than in the healthy state. Since the variability observed in correlation coefficients is very high in comparison with the one observed in static capacitance, it seems difficult to use the coefficient of correlation as a reliable indicator of PZT health. Thus, although the ERT allows for validating the presence of readable transmission throughout the testing sequence, different indicators might be sought for possible combinations for higher sensitivity to PZT bonding and repeatability. Other studies might aim at determining optimally relevant indicator variation threshold values.

5.2.5. Piezoelectric elements diagnostic procedure results after ageing

The healthy state is taken as the means of static capacitance of PZTs bonded on UPAT material in Healthy_ENSAM state. It can be noticed that the static capacitance between the healthy state and after the ageing test differs. It means that the PZT bonding becomes weaker after this experiment. However, the amplitude of the static capacitance decrease does not seem related to the ageing process duration. Indeed, the decrease is more important with the coupon L023 even if it stayed less time than coupon L023 (12-week vs 6 weeks). However, as results for only one coupon are available, general conclusions cannot be drawn here.

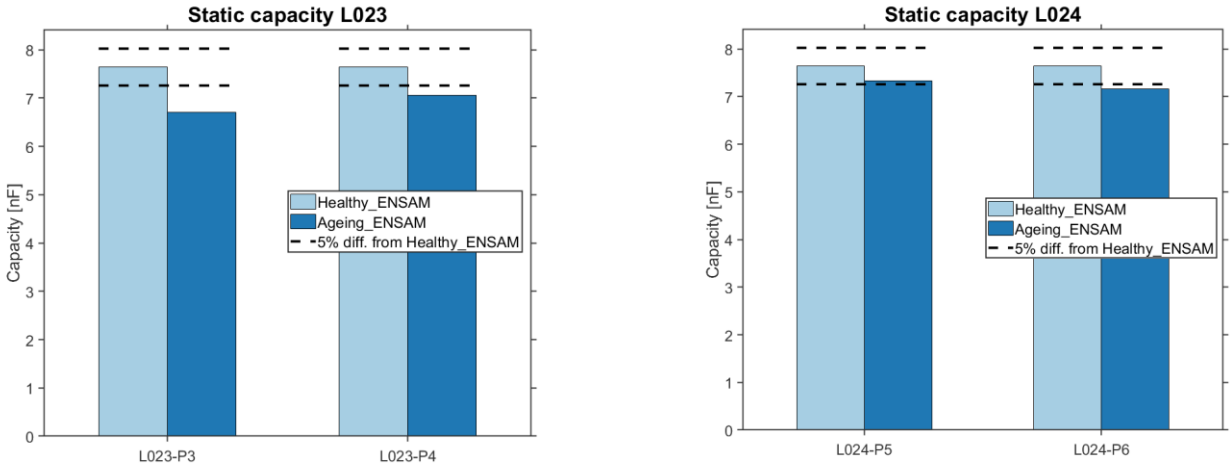

Figure 11: Static capacitance evolution after ageing (12 weeks on left and 6 weeks on right)

6. Optical fibers diagnostic

The OFs sensing technology should provide reliable measurements throughout their operational life where extensive degradation of their sensing capabilities must be avoided. The experimental campaign as presented in Sections 2 and 3 aims to describe the state of degradation under mechanical fatigue loading and ageing process and provide a threshold which will ensure reliable measurements.

In order to quantify the degradation and make a diagnosis of the operational state of the OFs the following process will be followed for the three test cases where the OFs are used.

The fatigue tests will be performed under displacement control in order to ensure that the longitudinal strain remains the same through the duration of the fatigue test. The strain will be measured every 1000 cycles and the following condition should be met:

$\varepsilon_{xx@intact\_phase} = \varepsilon_{xx@N*1000\ fatigue\ cycles}$, where $N = 1{:}300$. This condition should be true for both measurements via OF and digital image correlation.

In case that the L0 coupons experience damage due to fatigue loading, the strain measurement by OFs may be affected locally. Digital image correlation measurements will be affected as well and by comparing the differences between the strains acquired at different fatigue cycles from the two techniques, an assessment will be made if OFs or the L0 coupons are degraded.

Similar diagnostic procedure will be followed for analyzing the effect of ageing on the OFs measurement. The strain measurements between the different states of ageing should be same. In case the ageing degrades the L0 coupons, digital image correlation will benchmark this degradation.

TUD is in charge of OF testing. Results are not available at the moment of the redaction of this report.

7. Conclusion

Sensors reliability is a crucial issue in Structural Health Monitoring (SHM) and it is essential to ensure that sensors will function properly during the lifetime of the structure and do not jeopardize its integrity. Within this deliverable, the sensors and their connecting components have been subjected to realistic operational and environmental conditions to assess their reliability status. Sensorized coupons were analyzed in terms of stability and then submitted to repeated varying loads and temperature conditions as well as to ageing. Emphasis was given to the performance of bonding

between the sensors and the structure, as high-integrity bond should be maintained for in-service SHM systems. Two types of sensors have been under study: piezoelectric (PZT) and optical fibers (OF). Self-diagnostic capabilities were developed to monitor the performances of the PZT elements and to ensure that the sensors' output remained reliable. Measurement repeatability was used to assess OF correct bonding.

The results obtained are convincing and demonstrate that the chosen ReMAP bonding solution for both PZT and OF is adequate. This procedure can only provide improved results by using adhesives with higher thermomechanical coupling properties with the host structure.

8. References

[1] V. Giurgiutiu and A. N. Zagrai, "Embedded self-sensing piezoelectric active sensors for on-line structural identification," *Journal of Vibration and Acoustics-transactions of the ASME,* vol. 124, pp. 116-125, 2002.

[2] L. Yu and V. Giurgiutiu, Multi-mode Damage Detection Methods with Piezoelectric Wafer Active Sensors, Journal of Intelligent Material Systems and Structures, 2008.

[3] V. Pavelko, Application of the fatigue crack opening/closing effect for aircraft SHM, 7th International Symposium on NDT in Aerospace, 2015.

[4] E. Lizé, M. Rébillat, N. Mechbal and C. Bolzmacher, Optimal dual-PZT sizing and network design for baseline-free SHM of complex anisotropic composite structures, Smart Materials and Structures, 2018.

[5] G. Park, C. R. Farrar, A. C. Rutherford and A. N. Robertson, "Piezoelectric active sensor self-diagnostics using electrical admittance measurements," *Journal of Vibration and Acoustics-transactions of the ASME,* vol. 128, pp. 469-476, 2006.

[6] G. Park, C. R. Farrar, F. L. di Scalea and S. Coccia, "Performance assessment and validation of piezoelectric active-sensors in structural health monitoring," *Smart Materials & Structures,* vol. 15, pp. 1673-1683, 2006.

[7] S. Park, G. Park, C. B. Yun and C. R. Farrar, "Sensor Self-diagnosis Using a Modified Impedance Model for Active Sensing-based Structural Health Monitoring," *Structural Health Monitoring-an International Journal,* vol. 8, pp. 71-82, 2009.

[8] T. G. Overly, G. Park, K. M. Farinholt and C. R. Farrar, "Piezoelectric Active-Sensor Diagnostics and Validation Using Instantaneous Baseline Data," *IEEE Sensors Journal,* vol. 9, pp. 1414-1421, 2009.

[9] B. L. Grisso and D. J. Inman, "Temperature corrected sensor diagnostics for impedance-based SHM," *Journal of Sound and Vibration,* vol. 329, pp. 2323-2336, 2009.

[10] S. G. Taylor, G. Park, K. M. Farinholt and M. D. Todd, "Diagnostics for piezoelectric transducers under cyclic loads deployed for structural health monitoring applications," *Smart Materials and Structures,* vol. 22, 2013.

[11] Y. Zheng, C. Martinez, D. Easton, G. Park and K. Farinholt, "Sensor Self-Diagnostics for Piezoelectric Transducers Operating in Harsh Temperature Environments," in *Proceedings of SPIE Smart Structures and Materials & Nondestructive Evaluation and Health Monitoring Conference*, San Diego CA, 2011.

[12] J. L. Blackshire and A. T. Cooney, "Characterization of bonded piezoelectric sensor performance and durability in simulated aircraft environments," *Review of Progress in Quantitative Nondestructive Evaluation,* vol. 25, pp. 1694-1701, 2006.

[13] B. G. Falzon, K. A. Stevens and G. O. Davies, "Postbuckling behaviour of a blade-stiffened composite panel loaded in uniaxial compression," *Composites Part A,* vol. 31, no. 5, pp. 459-468, 2000.

[14] C. Meeks, G. Emile and F. G. Brian, "Stiffener debonding mechanisms in post-buckled CFRP aerospace panels," *Composites Part A,* vol. 36, no. 7, pp. 934-946, July 2005.

[15] K. A. Stevens, R. Ricci and G. A. O. Davies, "Buckling and postbuckling of composites structures," *Composites,* vol. 26, no. 3, pp. 189-199, 1995.

[16] A. C. Orifici, I. O. d. Z. Alberdi, R. S. Thomson and J. Bayador, "Compression and post-buckling damage growth and collapse analysis of flat composite stiffened panels," *Composites Science and Technology,* vol. 68, pp. 3150-3160, 2008.

[17] R. Degenhardt, A. Kling and K. Rohwer, "Design and analysis of composite panels," *III European Conference on Computational Mechanics Solids, Structures and Coupled Problems in Engineering,* 2006.

[18] S. Lauterbach, A. C. Orifici, W. Wagner, C. Balzani, H. Abramovich and R. Thomson, "Damage sensitivity of axially stringer-stiffened curved CFRP panels," *Composites Science and Technology,* vol. 70, no. 2, pp. 240-248, 2010.

[19] R. Krueger, J. G. Ratcliffe and P. J. Minguet, "Panel Stiffener Debonding Analysis using a Shell/3D Modeling Technique," *Composites Science and Technology,* vol. 69, no. 14, pp. 2352-2362, 2009.

[20] C. Bisagni, R. Vescovini and C. G. Davila, "Assessment of the Damage Tolerance if Post-Buckled Hat-Stiffened Panels using Single Stringer Specimens," *51st AIAA/ASME/ASCE/AHS/ASC Structures, Structural Dynamics, and Materials Conference, Structures, Structural Dynamics, and Materials and Co-located Conferences,* 2010.

[21] C. G. Davila and C. Bisagni, "Fatigue life and damage tolerance of postbuckled composite stiffened structures with initial delamination," *Composite Structures,* vol. 161, pp. 73-84, 2017.

[22] D. S. Zarouchas and R. C. Alderliesten, "The effect of disbonds on stability aspects of adhesively bonded aluminum panels during compression loading," *Thin-Walled Structures,* vol. 96, pp. 372-382, November 2015.

[23] "AMC 20-29, Composite Aircraft Structure, Annex II to ED Decision 2010/003/R of 19/07/2010, 2010".

9. Appendix: L-0 coupon card template

card n°	
Coupon	
Category	
Ref. Optimal	
Ref. CEDRAT	
Ref. ENSAM	

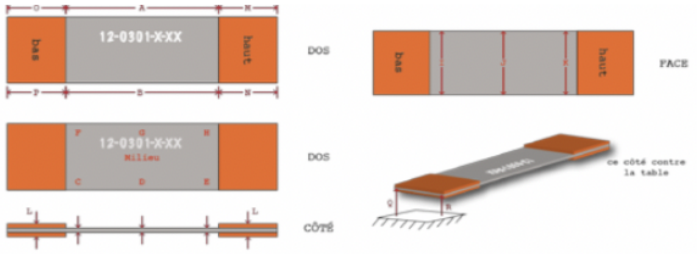

Dimensions, mm				Mass, g
A	*B*			
C	*D*			Plate material
E	*F*			
G	*H*			Tab material
I	*J*			
K	*L*			
M	*N*			

	Sensor 1	Sensor 2		
Ref. Manuf				
Ref. CTEC				
Dim (D x th), mm				
Mass, g				
Glue				
Glue protocol				
X, mm				
Y, mm				

Date/Time	Operator	Operation	Comment

10. Appendix: Piezo coupling for different composites

Dispersion curves calculated for different composite materials (ref UPAT, 2UPAT, EMB). Qualitatively, green represents high coupling, red represents low coupling. Patch diameter 20 mm.

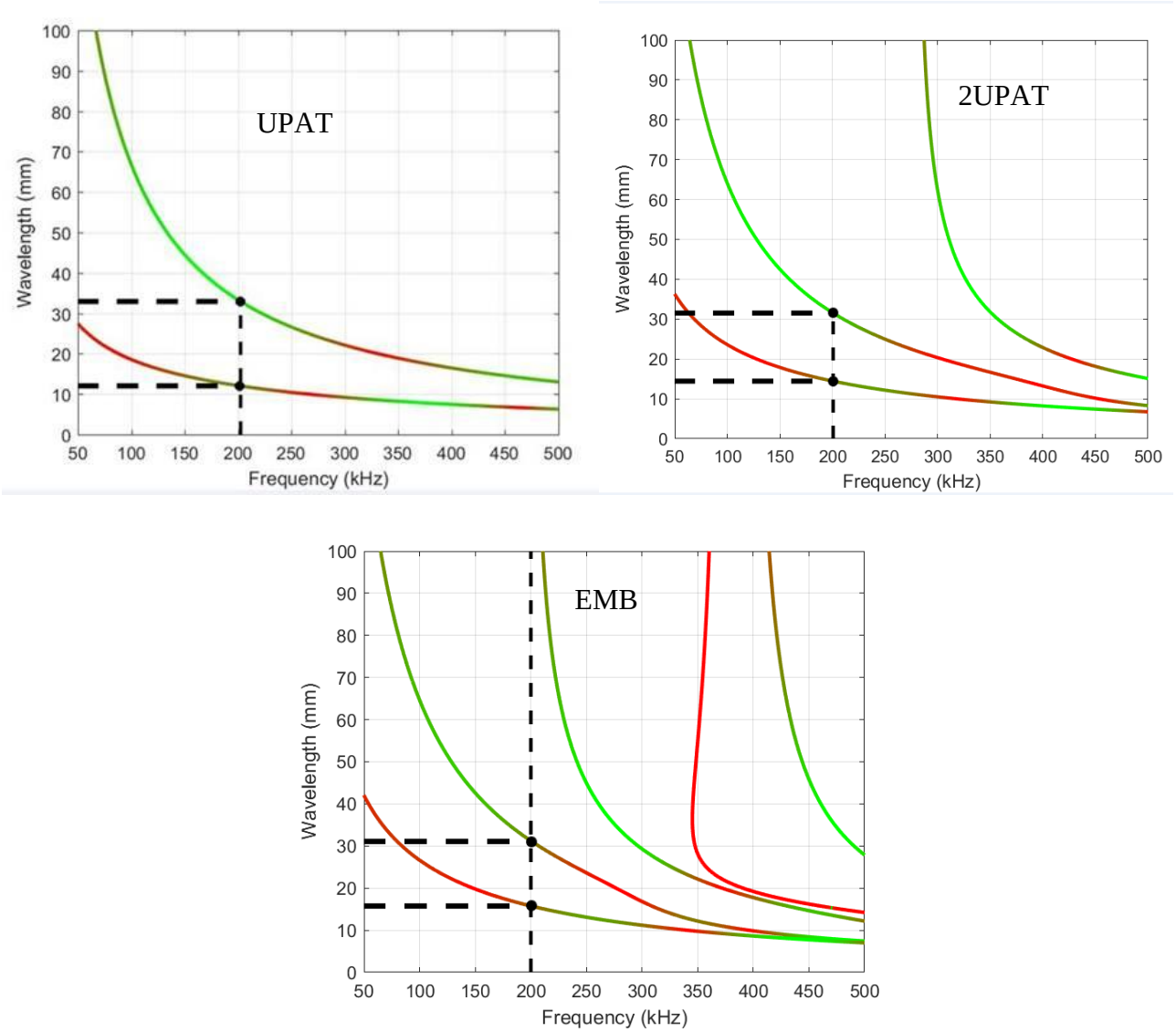

11. Appendix: Format to save EMT and ER data

11.1. Folder format:

NUMBER_STATE_ENTITY_DATE

Examples:

- 0_PZT_CTEC_141019 for tests before bonding
- 1_Healthy_CTEC_311019 for tests after bonding

11.2. Arborescence :

L101

```
├── 0_PZT_CTEC_161019
│   └── impedance
│
└── 1_Healthy_CTEC_311019
    ├── impedance
    │   └── Impedance_measurement_1V_1kHz_150kHz.mat
    └── 150kHz_5cycles
        ├── Actionneur1
        ├── Actionneur2
        ├── Actionneur3
        ├── Actionneur4
        ├── Actionneur5
        │   ├── measured_data_rep_1.mat
        │   ├── measured_data_rep_2.mat
        │   ├── measured_data_rep_3.mat
        │   ├── measured_data_rep_4.mat
        │   └── measured_data_rep_5.mat
        ├── Actionneur6
        ├── Actionneur7
        └── Actionneur8
```

11.3. Files format :

11.3.1. EMT :

File name : Impedance_measurement_ [LEVEL IN VOLT]V_[START FREQUENCY]kHz_[END FREQUENCY]kHz.mat

Example : Impedance_measurement_1V_1kHz_150kHz.mat

MATLAB file containing the structure **XP_SETUP** with the following fields :

name : 'impedance'

f_start : start frequency in Hz (ex : 1000)

f_stop : end frequency in Hz (ex : 150000)

level : level in Volt (ex : 1)

nb_points : number of frequency points (ex : 201)

nb_records : number of repetitions (ex : 2)

nb_active_channels : number of PZT (ex : 8)

freq_out : matrix containing the tested frequencies of size [NUMBER OF REPETITIONS] x [NUMBER OF PZT] x [NUMBER OF POINTS]

Exemple : 4 repetitions with 8 PZTs and 201 points should lead to a matrix of size 4x8x201

Z_out : impedance for all the tested répétitions of size [NUMBER OF REPETITIONS]x[NUMBER OF PZT]x[NUMBER OF POINTS]

11.3.2. ERT :

File name : measured_data_rep_[REPETITION NUMBER].mat (1 file per repetition)

MATLAB file containing the variable **data** of matrix type:

Column 1 : time

Column 2 : signal PZT 1

Column 3 : signal PZT 2

…

Column 9 : signal PZT 8

Column 10 : actuator commutation